Reactive Immunization

Peter Wirsching, Jon A. Ashley, Chih-Hung L. Lo, Kim D. Janda,* Richard A. Lerner*

For almost 200 years inert antigens have been used for initiating the process of immunization. A procedure is now described in which the antigen used is so highly reactive that a chemical reaction occurs in the antibody combining site during immunization. An organophosphorus diester hapten was used to illustrate this concept coined "reactive immunization." The organophosphonate recruited chemical potential from the immune response that resembled the way these compounds recruit the catalytic power of the serine hydrolases. During this recruitment, a large proportion of the isolated antibodies catalyzed the formation and cleavage of phosphonylated intermediates and subsequent ester hydrolysis. Reactive immunization can augment traditional immunization and enhance the scope of catalytic antibody chemistry. Among the compounds anticipated to be effective are those that contain appropriate reactive functionalities or those that are latently reactive, as in the mechanism-based inhibitors of enzymes.

The traditional process of immunization has been limited to the induction of noncovalent interactions between antigen and antibody. The discovery of antibody catalysis has resulted in another kind of antibody-antigen union (*1*). For example, efforts are directed toward the translation of binding energy into chemical modification of a substrate so that the nature of the interactions between antibody and antigen becomes as important as their energetics. At present, the mechanism and outcome of an antibody-catalyzed reaction have been controlled by synthesizing haptens endowed with geometric and electronic features modeling the transition state of the reaction. These compounds induce antibodies expected to stabilize attributes of the transition state as the substrate traverses the reaction coordinate, thereby lowering the energy of the reaction and increasing the rate. In spite of the successes, control over the mechanistic details of some reactions has remained elusive because the inherent randomness of the immune response precludes dictating how amino acids in the antibody combining site will participate in the mechanism of the reaction. Whereas transition-state energetics may remain a driving force in antibody catalysis, the incorporation of amino acid chemistry can augment and diversify its scope and complexity. Indeed, there have been rare and unexpected occurrences of such evolved, enzyme-like antibody behavior (*2*).

The selection of antibodies has now been made to occur as a result of bond-making and bond-breaking processes. We use reactive compounds as immunogens designed to promote specific chemistry in the antibody binding site, both in vivo during antibody induction and then later in catalysis. Thus, at the time of antibody-antigen encounter, a component of the binding energy results from complex chemical reactivity as well as from the simpler forms of complementarity dependent on electrostatic and hydrophobic forces. Therefore, it seems that a proportion of the responding B cell population reflective of such an additional interaction may predominate.

Structures anticipated to have desirable properties can be compared with mechanism-based inhibitors that inactivate enzymes. These compounds operate through interactions governed by functionalities in the active site and known to play a role in the catalytic sequence (*3*). However, such compounds may be viewed in the converse sense, in that a molecule that is capable of reactive inhibition of a mechanism will also be capable of inducing a similar mechanism. When the design of the immunogen requires an irreversible chemical reaction, the immunization can be considered to transpire via a covalent process.

Principle and design. If reactive compounds are considered as haptens, there must be sufficient reactivity to undergo chemical reactions in the binding site of the antibody, but not too much lability to be completely degraded by the many chemical entities encountered in vivo during immunization. Also, the compounds chosen must be stable enough to allow adequate conjugation to a carrier protein to form the immunogen.

An organophosphonate diester structure was chosen as a model for reactive immunization (Scheme 1) because it could provide a test of principle and it could provide insight into the nature of phosphonylated enzymes and the recruitment of their catalytic activity (*4*–*6*). Also, stability could be modulated, depending on the electronic nature of the aryl rings, and possible structural modifications could be explored by disrupting the symmetry of the compound. However, there was the possibility of a double selection between two haptens: the starting diester which was very reactive, and the other a stable transition-state analog, which increased in concentration as a result of hydrolytic decomposition during the immune response (Scheme 1); such interaction between these two could affect the chemical and catalytic attributes of antibodies. Structure-reactivity studies suggested that the paramethylsulfonyl (*p*-SO_2Me) analog **1** (Fig. 1 and Table 1) would survive immunoconjugation procedures, would have an adequate lifetime in vivo, yet offered enough reactivity to interact chemically with immunoglobulins (*7*).

Under the coupling conditions for hapten **1**, it was estimated that immunization began with a mixture of equal amounts of each immunogen, such as **2** and **10**, and that the antibodies derived from them would be a result of the interplay between these two immunogens (*8*). The end result would then be a cross-reacting immune serum with a reduced affinity for both haptens, a higher affinity for **10** relative to **2**, and the installation of chemical reactivity.

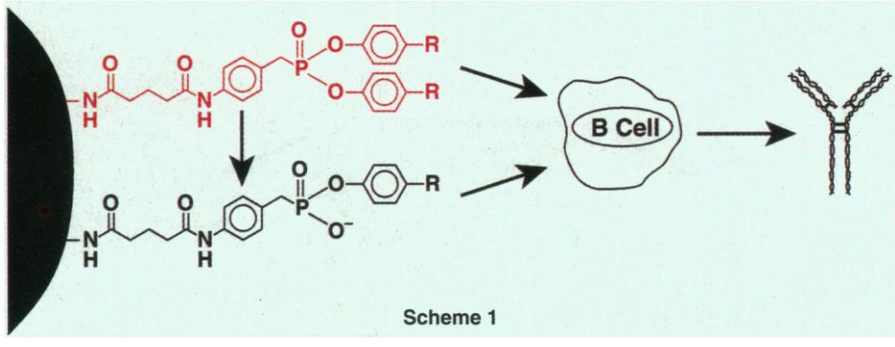

Scheme 1

The authors are at the Scripps Research Institute, Departments of Molecular Biology and Chemistry, 10666 North Torrey Pines Road, La Jolla, CA 92037, USA.

*To whom correspondence should be addressed.

A panel of 19 monoclonal antibodies (mAbs) was obtained for analysis (9). Complete assessment of the reactive immunization hypothesis required the examination of the characteristics of the entire collection. The dissociation constants (K_d) of **12** were determined by fluorescence quenching or with ^{3}H-labeled **13** by equilibrium dialysis (Table 2) (*10*). In that the diester **5** decomposed in solution and gave **12**, we were unable to differentiate unequivocally the binding between these two compounds under equilibrium conditions. Hence, to demonstrate that an uncharged, *p*-SO_2Me-phenyl phosphonate ester bound to these antibodies, we used the stable analog **16** as a surrogate for **5** and obtained approximated K_d values (Table 2) (*11*). These data provided an upper limit on K_d because the binding energy that might be afforded by an additional *p*-SO_2Me-phenyl ring was absent. However, it was expected that ^{3}H- or ^{14}C-labeling could distinguish those antibodies that reacted rapidly, covalently, and stoichiometrically, or perhaps where reaction was not as rapid, but where the diester was thermodynamically competitive with **13**. Incubation of SPO monoclonal antibodies with an excess of **7** or **8** indicated, in a number of cases, that one equivalent of ^{3}H- or ^{14}C-label remained bound to the protein even after extensive dialysis. Yet, in denaturation experiments designed to establish covalent as opposed to noncovalent binding, either little or no radioactivity remained associated with the protein (*12*), an indication that kinetic phenomena were operative.

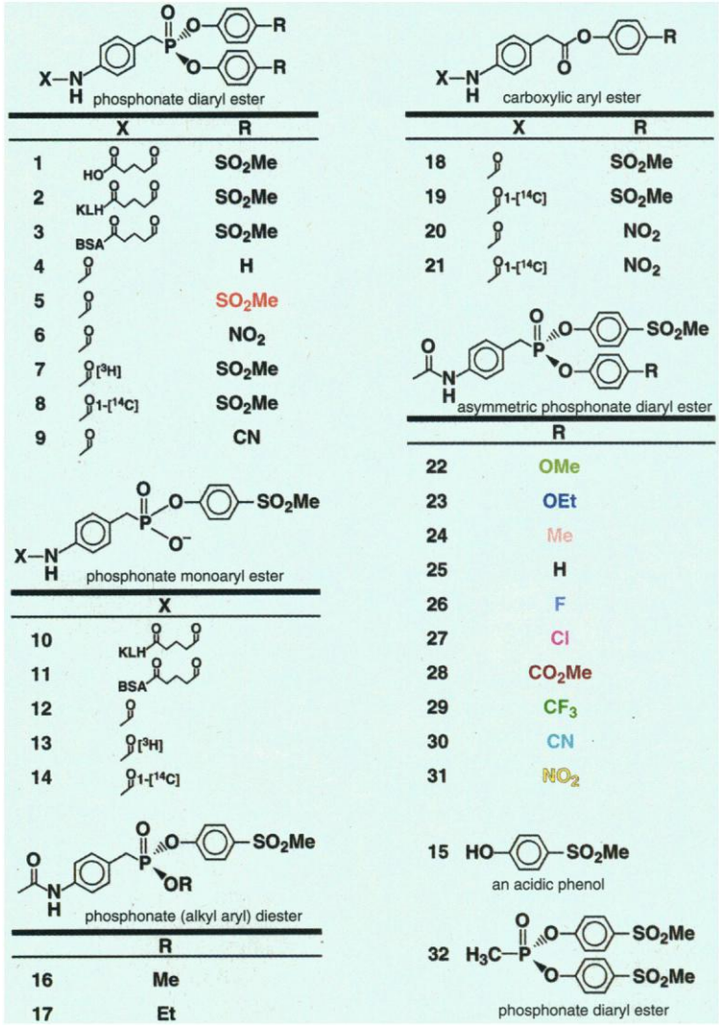

Fig. 1. Structures and numerical assignments of compounds.

Kinetics and mechanism. An antibody phosphonylated with **5** could (i) dephosphonylate and possibly reactivate by cleavage of the phosphorus-protein bond (A), (ii) age by hydrolysis of the other phosphonate ester from which no reactivation occurs (B), or (iii) react through a combination of both pathways (*13*) (Scheme 2). To study the inactivation kinetics of the SPO family with **5** as a substrate, we used high concentrations of antibody under pseudo first-order conditions. Both possible products of the reaction, **12** and **15**, were then simultaneously subjected to high-performance liquid chromatography (HPLC) (*14*). The relative rates of phosphonylation, dephosphonylation, and aging were then evaluated. Members of the SPO panel showed that 11 of the 19 antibodies catalyzed the hydrolysis of **5** compared to the background, buffer-catalyzed reaction (Table 2); in most cases, this resulted in a one-turnover inactivation of the antibody. Unexpectedly, the putative phosphonyl intermediates were usually labile, with dephosphonylation the predominant mode of reaction. This lability explained the results obtained in ^{14}C-labeling experiments with **8**. However, dephosphonylation rarely led to reactivation because the reaction product **12** was often a tight-binding, competitive inhibitor (**13**, in Table 2). The reactivity of these intermediates was quite a contrast to that observed for inactivated serine esterases and proteases (*13*). Perhaps most interesting was the behavior observed with regard to the rates and pathways during the inactivation process that resulted from phosphonylation, dephosphonylation, and aging reactions.

The most studied antibody was SPO49H4. When an excess of **5** was rapidly mixed with the antibody, the buildup of products was greater than 60 percent within the mixing time and increased until approximately one

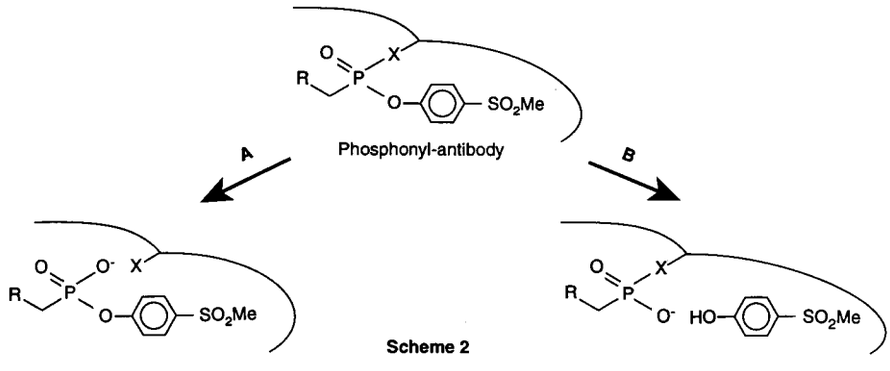

Scheme 2

equivalent of each was produced (Fig. 2A). Moreover, the rates of formation of **12** and **15** were the same, an indication that there was no significant accumulation of an intermediate and that phosphonylation was largely rate determining (*15*). The progress curves gave an observed first-order rate constant for inactivation of 6.4 min^{-1} (*16*). If k_{obs} gives an estimate of the rate of phosphonylation and sets a lower limit on the rate of dephosphonylation, then k_{obs} approximates the first-order rate constant for inactivation (k_{inact}). In essence, **5** could be viewed as a mechanism-based inhibitor of SPO49H4 where the time-dependent loss of activity was monitored directly and where the partition ratio was essentially zero. At comparable micromolar concentrations of antibody and inhibitor in the range of the K_d, complete inactivation occurred within 10 minutes (Fig. 2A, inset). A measure of the potency of inactivation is indicated by the apparent second-order rate constant of inactivation, k_{inact}/K_d (K_d for **16**), which is analogous to k_{cat}/K_m for a true substrate. This gave a value of 4.7×10^5 M^{-1} min^{-1}. Although inactivation of acetylcholinesterase and serine proteases by nonspecific organophosphonofluoridates and chloridates occurs near the diffusion limit, the inactivation of the antibody by **5** is only about 10 times slower than inactivation of serine proteases by peptidic phosphonate diphenyl esters (*5*) and about 100 times faster than inactivation of these enzymes by many peptidomimetic phosphonate monoesters (*4*).

Although the reaction course of phosphonylation was programmed by hapten design of **1**, the antibody must have resulted from reactive immunization under the influence of electrostatic interactions provided by **10**. A priori, we would not expect that the process of selection for phosphonylation would also be the sole driving force that afforded rapid dephosphonylation. Possible evidence for the influence of **10** arose when it was discovered that many of the antibodies used the activated ester **18** in a highly specific and catalytic fashion (Table 2). The most efficient among these was SPO49H4, where the ratio of k_{cat} to K_m was 1.0×10^5 M^{-1} min^{-1}. We estimated that turnover of the antibody was limited only by the rate of product release. There was no significant pre–steady-state accumulation of an intermediate although an acyl antibody could be trapped at low pH in a stoichiometric amount (*17*). The competency of this substrate suggested that both covalent catalysis and transition-state stabilization were operative. In particular, the acylation with **18** substantiated the presence of an antibody nucleophile and, hence, the existence of a phosphonyl intermediate. Furthermore, features of the active site derived from selection by **10** could be implicated in the antibody chemistry with phosphonate diesters. The impact on catalysis is likely to be electrophilic because of the formation of an "oxyanion hole" common in antibody catalysis (*18*). Using *p*-cresol and compound **24** as models for an antibody intermediate operating by way of a tyrosyl residue, we estimated that SPO49H4 offered a 60,000 times greater advantage in the formation of the phosphonyl-antibody and at least a factor of 1×10^6 in its hydrolysis (*19*). Finally, our data suggested that binding interactions by the *p*-SO_2Me group played a significant role in the observed kinetics. The more reactive nitro analog **20** was a slow substrate for SPO49H4, whose

Table 1. Hydrolytic stabilities of some hapten-like compounds. For each compound, the buffer-catalyzed first-order rate constant (k_{hyd}) was determined under the following conditions: (A) 100 mM Bicine, pH 8.0, 5 percent DMF in 5 percent CH_3CN cosolvent at 22°C; (B) 100 mM phosphate, pH 7.4, 5 percent DMF in 5 percent CH_3CN cosolvent at 22°C; (C) 50 mM phosphate, pH 7.5, 5 percent DMF in 5 percent CH_3CN cosolvent at 4°C. For all compounds, values were determined by means of HPLC, except for **6**, which was determined spectrophotometrically [ε_{404} for (A) = 15,700 M^{-1} cm^{-1}, ε_{404} for (B) = 13,000 M^{-1} cm^{-1}]. HPLC for **1** and **5** followed the formation of **15** as described (*14*). For **4**, formation of the monophenyl ester product was followed with an isocratic mobile phase of 8 percent CH_3CN and 92 percent water (0.1 percent trifluoroacetic acid) at 2.0 ml/min. ND, not done.

Compound	k_{hyd} (min^{-1})		
	A	B	C
1	ND*	ND	4.8×10^{-4}
4	5.0×10^{-6}	2.3×10^{-6}	ND
5	5.13×10^{-4}	9.6×10^{-4}	6.4×10^{-4}
6	1.3×10^{-3}	1.1×10^{-2}	ND

*ND, not determined

Table 2. Kinetic and thermodynamic parameters for SPO mAbs.

SPO mAb	IgG isotype	K_d (**16**)* (μM)	K_d (**13**)† (μM)	k_{obs} (min^{-1})‡		k_{cat} (**18**)§ (min^{-1})
				12	**15**	
49H4	$\kappa\gamma_{2a}$	3.0	0.11	6.4	6.4	31‖
71A7	$\kappa\gamma_1$	0.20	0.17	0.080¶	0.087	5.1
79D12	$\kappa\gamma_{2b}$	0.20	0.14	0.18#	0.18	2.6
13F8	$\kappa\gamma_1$	5.0	0.074	0.16**	0.11	0.025††
50A5	$\kappa\gamma_{2a}$	0.20	0.10	ND‡‡	0.012	0.047
45G6	$\kappa\gamma_{2b}$	0.92	6.0	0.0039§§	0.0018	0.076
56C4	$\kappa\gamma_{2b}$	1.3	9.6	ND	0.0010	0.17
50C1	$\kappa\gamma_1$	0.10	0.068	ND	0.017	78‖‖
87E2	$\kappa\gamma_{2a}$	0.10	0.83	0.069	0.069	0.0058
87B2	$\lambda\gamma_1$	2.0	5.0	0.0042¶¶	0.0023	0.028
89E11	$\kappa\gamma_{2a}$	2.0	3.6	0.015##	0.012	0.046
96G2	$\lambda\gamma_1$	2.0	1.3	ND	ND	0.25
91B4	$\lambda\gamma_1$	0.15	1.4	ND	ND	0.21
40C11	$\kappa\gamma_{2a}$	0.40	0.64	ND	ND	0.18
50A10	$\kappa\gamma_{2a}$	0.30	3.5	ND	ND	0.14
38F10	$\kappa\gamma_1$	2.0	0.17	ND	ND	0.10
34B11	$\kappa\gamma_1$	0.50	0.078	ND	ND	ND
52D1	$\kappa\gamma_1$	0.10	0.10	ND	ND	ND
82D2	$\kappa\gamma_{2b}$	1.0	15	ND	ND	ND

*Determined by fluorescence quenching (*10*). †Determined by equilibrium dialysis (*10*). ‡Determined under the reaction conditions and HPLC analysis described (*14*). In each case, 40 μM mAb and 700 μM **5** were used. The k_{obs} were the observed first-order rate constant for product formation in which inactivation resulted from either dephosphonylation, aging, or both, except where indicated. All data were fit with the equation in (*16*). When possible, the true first-order rate constants for dephosphonylation (k_r) and aging (k_a) were estimated from the relation, k_{obs} (**12**) = $k_r + k_a$ and k_r/k_a = (percent **12** formed)/(100 − percent **12** formed). §Determined under the reaction conditions and HPLC analysis described (*14*), except where indicated. In each case, 20 μM mAb and 250 μM **18** were used. This concentration of **18** was saturating. The buffer-catalyzed first-order rate constant for hydrolysis of **18** was 4.62×10^{-3} min^{-1}. The background rates were subtracted from the mAb-catalyzed rates. ‖The parameters for SPO49H4, SPO71A7, and SPO79D12 were determined spectrophotometrically as described (*20*) in the presence of 0.20 μM or 1.0 μM mAb, and by varying the concentration of **18**. The data were fit hyperbolically (*39*). K_m (49H4) = 300 μM; K_m (71A7) = 67 μM; K_m (79D12) = 101 μM. ¶k_r = 0.060 min^{-1}, k_a = 0.016 min^{-1}; 20 percent aging. #Slow turnover (0.2 μM/min) continued up to 1.25 equivalents of product formation. **k_r = 0.14 min^{-1}, k_a = 0.016 min^{-1}; 10 percent aging. ††For SPO mAbs 13F8, 56C4, 87E2, 87B2, and 89E11, there was a one equivalent formation of **15** with no significant steady-state rate up to 35 percent substrate depletion. ‡‡Nd, none detected. The amount of product formation was within experimental error (±10 percent) of background. §§k_r = 0.0019 min^{-1}, k_a = 0.0019 min^{-1}. ‖‖The burst formation of one equivalent of **15** was determined by means of stopped-flow spectrophotometry (Hi-Tech Scientific), 0.2-ml cell, 1-cm path length, 0.2-ml stop-volume, 266 nm; 2 μM mAb, 25 μM **18** with conditions described (*20*). There was no detectable steady-state rate. ¶¶k_r = 0.0011 min^{-1}, k_a = 0.0031 min^{-1}; 75 percent aging. ##Estimated from less than one equivalent of **15**. The ratio of the concentration of **12** to that of **15** was 0.33.

k_{cat} was 7 percent that of **18**, did not show burst kinetics and could not be ^{14}C-labeled with **21**. This could be explained by a changeover to acylation as the rate-determining step.

The ester substrate **18** permitted investigation of the inactivation of SPO49H4. The incubation of antibody, **5**, and **18** resulted in time-dependent loss of catalytic activity when the reaction was continuously monitored for release of **15** at 266 nm (*20*). Progress curves, generated from several concentrations of inhibitor and fixed amounts of substrate and antibody (Fig. 2B), were fit by nonlinear least-squares analysis (*16*). The values of k_{obs} and the initial velocities showed a hyperbolic dependence on the concentration of **5** (Fig. 2B, inset, and C). The data could therefore be interpreted from the minimal model for mechanism-based inhibition in the presence of a competing substrate and where the partition ratio approaches zero (Scheme 3) (*21*). In this scheme, E represents the antibody, EA a reversible complex with **18**, EI a reversible complex with **5**, EI′ a phosphonylated antibody, EX the final inhibited complex with **12** and **15**, and A and P are **18** and **15**, respectively. The rate constant k_5 approximates k_{inact} when it is the rate-determining step. The data, which were in accord with our direct assessment of inactivation, provided a value for the inhibition constant K_i which compared with the K_d value approximated by **16** (Table 2). The agreement between K_i and K_I was further indication that k_5 controlled the rate of inactivation. Finally, the k_{cat} for **18** of 35 min^{-1} was consistent with that found previously (Table 2) and supports the applicability of the kinetic scheme.

Other members of the SPO family displayed characteristic behavior and exemplified the diversity available from reactive immunization. In particular, the observed difference in the rates and amounts of formation of **12** and **15** for some antibodies gave direct evidence for the partitioning from a phosphonyl-antibody intermediate.

The reaction of SPO56C4 with **5** represented a case where there was no significant production of **12** and therefore an extremely slow rate of dephosphonylation. However, the liberation of two equivalents of **15** was observed (Fig. 3A). The extra **15** was not a result of antibody turnover given the absence of formation of **12**. Hence, the additional equivalent came from the aging of a covalent intermediate. The apparent first-order rate constant for formation of **15** is a function of the true first-order rate constants for phosphonylation and aging. If these are of similar magnitude, a value of $k_{app} = 0.060\ hr^{-1}$ can be assigned to these steps (*22*) and compared to the rate constants for hydrolysis of **17** and **24** used as models for antibody intermediates of serine or tyrosine, respectively. These comparisons suggested a rate enhancement of 2700 and 230 times faster for the phosphonylation step and aging reaction, respectively, invoking serine, and 10 and 28 times faster for that of tyrosine (*19*, *23*). It is clear that SPO56C4 is a poor catalyst of its own inactivation and that its rate and pathway of reaction differ from those of SPO49H4.

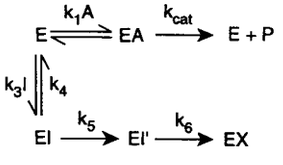

Scheme 3

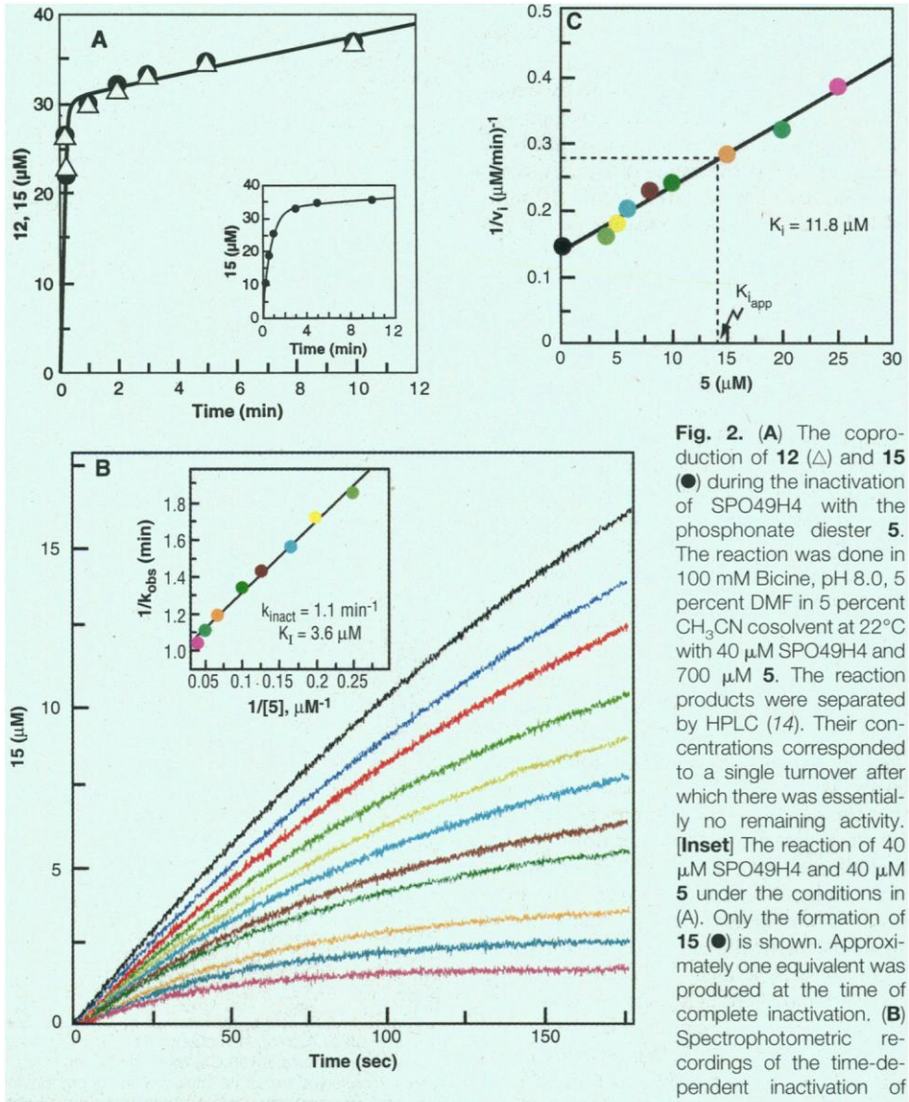

Fig. 2. (**A**) The coproduction of **12** (△) and **15** (●) during the inactivation of SPO49H4 with the phosphonate diester **5**. The reaction was done in 100 mM Bicine, pH 8.0, 5 percent DMF in 5 percent CH_3CN cosolvent at 22°C with 40 μM SPO49H4 and 700 μM **5**. The reaction products were separated by HPLC (*14*). Their concentrations corresponded to a single turnover after which there was essentially no remaining activity. [**Inset**] The reaction of 40 μM SPO49H4 and 40 μM **5** under the conditions in (A). Only the formation of **15** (●) is shown. Approximately one equivalent was produced at the time of complete inactivation. (**B**) Spectrophotometric recordings of the time-dependent inactivation of SPO49H4 with **5** monitored at 266 nm by the release of **15** from the substrate **18**. The reactions were done in 100 mM Bicine, pH 8.0, 5 percent DMF in 5 percent CH_3CN cosolvent at 22°C with 1.0 μM SPO49H4, 75 μM **18**, and varying concentrations of **5** (*20*). The concentrations of **5** (beginning at the top) were: (black) 0 μM; (blue) 1.0 μM; (red) 2.0 μM; (green) 4.0 μM; (yellow) 5.0 μM; (cyan) 6.0 μM; (purple) 8.0 μM; (dark green) 10 μM; (orange) 15 μM; (aqua) 20 μM; and (magenta) 25 μM. The progress curves were fit by the equation in (16) from 180 data points. The 0, 1, and 2 μM data were not included in calculations. (**Inset**) The double-reciprocal representation of the hyperbolic dependence of the observed first-order rate constants on the concentration of **5**. The values of k_{inact} and K_I were derived from the reciprocals of the *y* intercept and *x* intercept, respectively. (**C**) Dixon plot of the initial velocities obtained from the progress curves in (B) with respect to the concentrations of **5**. The concentrations of **5** (beginning at the left) were: (black) 0 μM; (green) 4.0 μM; (yellow) 5.0 μM; (cyan) 6.0 μM; (purple) 8.0 μM; (dark green) 10 μM; (orange) 15 μM; (aqua) 20 μM; and (magenta) 25 μM. The data were fit by linear least-squares analysis. The K_I was determined from K_{iapp} using the relationship $K_{iapp} = K_I(1 + [S]/K_m)$. The dotted line is drawn from a *y*-intercept = $2(1 + K_m/[S])/V_{max}$ where S is compound **18**.

These differences may result from a weak electrostatic potential at the active site with reactivity arising only from minor entropic gains because SPO56C4 binds **12** nearly two orders of magnitude less tightly than SPO49H4. SPO50A5 also aged completely, but ten times faster, while subtle effects in other antibodies made them susceptible to both dephosphonylation and aging (Table 2). The antibody SPO45G6 showed the most complex behavior and illustrated all possible concurrent events (Fig. 3B). Because the antibody generated one full equivalent of **12**, but three equivalents of **15**, it must have undergone one-and-a-half turnovers (two phosphonylations) and complete aging before inactivation. Apparently, binding of **5** was competitive with **12** so that inactivation did not result after one dephosphonylation event. If aging were not a factor, additional turnovers and more of **12** might have resulted. Final confirmation of phosphonyl-antibody intermediates and the aging hypothesis was obtained from ^{3}H-labeling (*24*).

The kinetic behavior of the SPO monoclonal antibodies support a mechanism whereby phosphonyl intermediates, whether in enzymes or immunoglobulins, can utilize the chemical potential of an oxyanion hole. In the reactions of serine hydrolases, reactivation and aging are slow, but occur more readily for aryloxy leaving groups, as opposed to alkoxy ligands, which lock the enzyme in an inappropriate protonation state for hydrolysis (*25*). For the antibodies, the magnitude of the electrostatic interaction and the orientation of the intermediate with respect to the anionic binding site may govern the rates and pathways of phosphonylation, dephosphonylation, and aging. The effect of this site either may be minimal in that it was elicited only from the charge separation of the P-O double bond in **1** or the covalent intermediate, or it may be stronger through interplay with **10** during selection. However, in the formation and cleavage of a covalently bound phosphonyl intermediate, some antibodies, compared to enzymes, can make efficient use of a simpler mechanism. The organophosphorus inhibitors recruit almost the full catalytic power of serine hydrolases during phosphonylation, but this catalytic machinery becomes an impediment in the dephosphonylation reaction, suggesting that the phosphonyl intermediate may be a model for the deacylation step of these enzymes (*26*). In the recruitment of catalytic power, the SPO monoclonal antibodies work freely between acyl and phosphonyl intermediates (or tetrahedral and pentavalent transition states). SPO49H4 operates equally well with **5** or **18** (compare k_{inact}/K_i with k_{cat}/K_m), but, as is often the case in antibody catalysis, the reactions were encumbered by product binding steps.

Structure and mechanism. Much of the catalytic potential of SPO49H4 arose from, and resided in, the binding energy of the *p*-SO_2Me phenyl ring. The strong product binding and the slow rate of product release contributed to efficient inactivation and prevented it from being a more proficient catalyst. The high affinity and specificity for the *p*-SO_2Me group were therefore used to seek further evidence for the existence of a phosphonyl-antibody intermediate.

The Hammett rho sigma ($\rho\sigma$) and related studies have been useful in enzymology and, in particular, the kinetic and chemical mechanisms of serine protease and esterase catalyses were supported with such linear free energy relationships (*27, 28*). Substituent effects on an antibody-catalyzed hydrolysis of phenyl esters gave evidence for an acyl-antibody intermediate (*29*). However, only a few Hammett-type investigations in which organophosphorus compounds were used have been reported (*30*). The hydrolysis of ten mixed-ester phosphonates, **22** to **31** (Fig. 1), was examined with and without catalysis by SPO49H4 (*31*). High-performance liquid chromatography (HPLC) was used to determine the buffer-catalyzed rate of formation of **12** and **15**, the overall pseudo first-order rate constant (k_{hyd}), and k_{obs} for the inactivation of SPO49H4 (*32*). Excellent correlation (r = 0.973) was obtained for k_{hyd} assessed as a function of the original Hammett σ constants (*33*). The correlation for production of **12** or **15** were also good (r = 0.94–0.96). In that the interplay between substituents on the two aryl rings determined the reactivity of each compound, log k_{hyd} was used for correlation with σ and gave ρ = 1.02 (Fig. 4A). In all cases, the hydrolytic partitioning of the diesters favored generation of **15** and the corresponding para-substituted phosphonic acid (*34*). The antibody alone catalyzed the formation of **12** and the para-substituted phenol (*35*). When log k_{obs} for the antibody reactions was plotted as a function of σ, the Hammett relation was satisfied and afforded ρ = 2.14 (Fig. 4B). The observed substrate selectivity and the $\rho\sigma$ correlation, taken together, support the case for covalent catalysis.

1) Evidence from inactivation experiments indicated that for a mechanism that operated through a phosphonyl intermediate, the phosphonylation step was largely rate-determining. If the substituent effects on k_{obs} measured substituent effects on phosphonylation, and if all of the substrates phosphonylated the antibody by the same mechanism through a common intermediate, a linear free energy relation should ensue. Furthermore, a value of 2 for ρ is indicative of the development of substantial charge in the transition state for release of the respective phenols. Hydrolysis of acyl phenyl esters via a general-base mechanism is characterized by little charge buildup on the phenolic oxygen and thus a low ρ value of 0.5 to 0.7, whereas attack by hydroxide usually results in somewhat higher ρ values of 1 to 1.2 (*36*). This is consistent with the ρ value of 1.02 for the buffer-catalyzed reaction and with hydrolysis of other organophosphorus esters (*30*), but not with the value found for the antibody-catalyzed reaction. A mechanism invoking an antibody

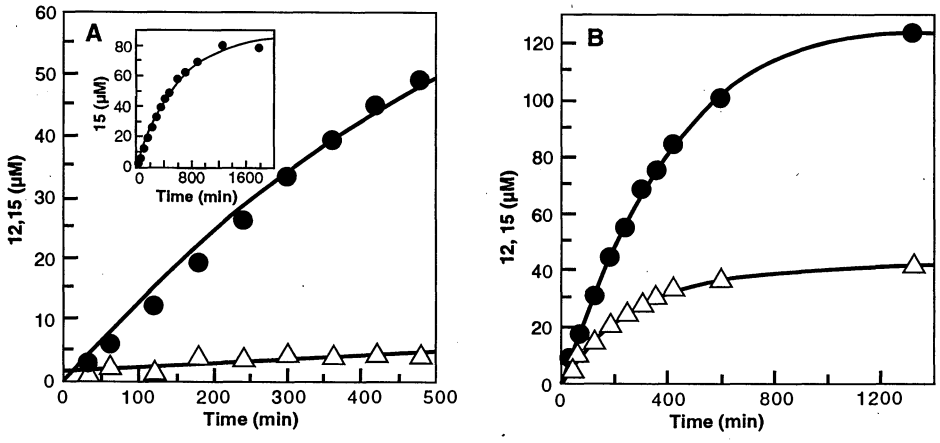

Fig. 3. (**A**) The partial time course for the formation of **12** (△) and **15** (●) during the inactivation of SPO56C4 with the phosphonate diester **5**. The reaction was done in 100 mM Bicine, pH 8.0, 5 percent DMF in 5 percent CH_3CN cosolvent at 22°C with 40 μM SPO56C4 and 700 μM **5**. The reaction products were separated by HPLC (*14*). The concentrations of **12** fluctuated within experimental error (±10 percent) of background values. (**Inset**) The full time course for the formation of **15** during the inactivation of SPO56C4 with **5**. The conditions were as in (A). The final concentration corresponded to the production of two equivalents of **15**. (**B**) The formation of **12** (△) and **15** (●) during the inactivation of SPO45G6 with the phosphonate diester **5**. The reaction was done in 100 mM Bicine, pH 8.0, 5 percent DMF in 5 percent CH_3CN cosolvent at 22°C with 40 μM SPO45G6 and 700 μM **5**. The reaction products were separated by HPLC (*14*). The final concentration of **12** corresponded to approximately one equivalent, and that of **15** to nearly three equivalents compared to the concentration of antibody.

nucleophile could account for the ρ value found in our experiment (*37*). Nucleophilic addition to phosphorus in the SPO49H4 active site during the phosphonylation step proceeded through a later transition state with more charge development, and therefore it was more sensitive to the electronic effects of substituents.

2) As shown above, the antibody completely reversed the chemoselectivity of the hydrolysis, and thus met a disfavored free energy barrier. On the basis of reactivity, simple hydroxide catalysis should have produced only **15** and the respective phosphonic acid in all cases. The geometry and energetics of nucleophilic attack require the leaving and entering groups to be on opposite sides of a plane that bisects the phenolic aryl groups through the phosphorus atom (Scheme 4). In an in-line, single-displacement mechanism where the substrate lies in the active site, attack by a nucleophile from the exterior of the protein would produce the thermodynamically favored products (*38*). Because of the observed outcome, it is more plausible that the antibody hydrolyzes the phosphonates through a covalent intermediate by a double-displacement mechanism. This way, substrate binding energy and an amino acid nucleophile lower transition-state barriers for phosphonylation at a minimal cost of negative entropy.

As discussed above, SPO49H4 was very specific for the *p*-SO_2Me moiety and produced the less acidic phenol. Because the compounds **22** to **31** are chiral, it was possible to examine the enantioselectivity of diester hydrolysis. When excess antibody (50 μM) reacted with **24** (20 μM), the reaction only proceeded to 50 percent completion. Then, it was possible to infer that 10 μM of one enantiomer of **24** remained in solution. In essence, SPO49H4 effected a stoichiometric "thermodynamic" resolution.

Finally, since coproduction of the products **12** and **15** resulted from the hapten-like substrate **5**, a disruption of this finely tuned binding may afford an observable separation of the two-step process of phosphonylation and dephosphonylation. The less hapten-congruent compound **32** was a substrate for the antibody and also led to its inactivation. However, in this case, there was a lag time in the production of the phosphonic acid, an indication of the intermediacy of a phosphonyl-antibody. Apparently, loss of binding interactions by removal of the 4-acetamidophenyl fragment resulted in a less precisely oriented covalent intermediate so that hydrolysis of the intermediate was slower than its formation on a macroscopic time scale. Although the rate of product formation was reduced compared to **5**, the antibody turned over and liberated 2.6 equivalents of **15**, but only 2.2 equivalents of the corresponding phosphonic acid, before complete inactivation resulted. Hence, this intermediate, unlike the intermediate formed with **5**, was susceptible to aging.

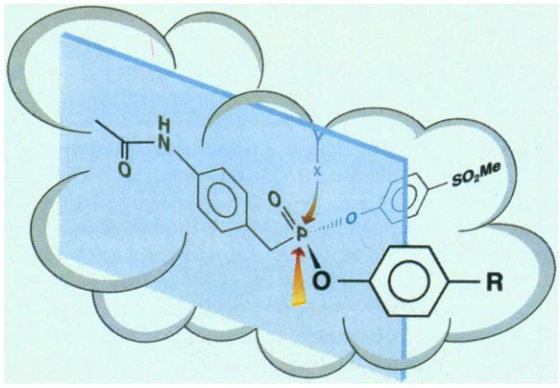

Scheme 4

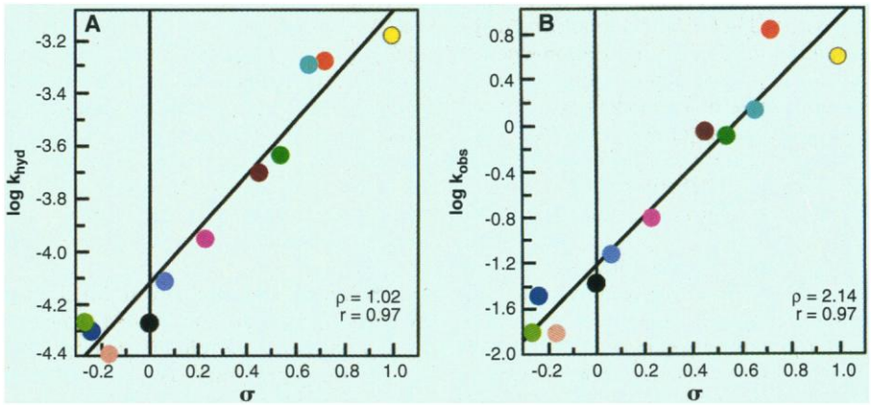

Fig. 4. (**A**) Hammett plot of the buffer catalyzed pseudo first-order rate constants for the hydrolysis of **5** and **22** to **31** with respect to the original σ constants (*27, 33*). (**B**) Hammett plot of the observed first-order rate constants for the inactivation of SPO49H4 with compounds **5** and **22** to **31** with respect to the original σ constants (*27, 33*). For both (A) and (B), the reaction conditions and HPLC analyses were as described (*14, 32*). The colors correspond to the color coded substituents in Fig. 1, and the ρ value equaled the slope of the line calculated from a linear least-squares fit that had the indicated correlation coefficient.

Enzymes and immunization. Immunization should no longer be limited to eliciting antibodies on the basis of tight binding to a preconceived antigen. A more dynamic approach that enlists chemical reactivity offers the opportunity to enhance the power of immunization and to harvest any kind of protein from the immune response; accordingly, a chemical reaction can be used as part of the process of antibody induction. Such a change is a departure from conventional procedures of selection by generation of noncovalent interactions that leave the antigen and antibody chemically unaltered.

In principle, any reactive compound or mechanism-based inhibitor may be used to generate antibodies so long as the compound has sufficient lifetime during immunochemical protocols. A large number of mechanism-based inhibitors are already available and many of them could be used to expand the scope of antibody catalysis. On the basis of our results, catalysts produced from covalent reactions between immunogen and immunoglobulin can be highly efficient and establish a link with the mechanisms of enzymes. In addition, cross-reactivity, which is usually undesirable and detrimental in traditional immunization, can be used to advantage in reactive immunization. Hence it may be possible to bring reactive species together at the antibody combining site and approximate what enzymes do in multisubstrate reactions or when using high-energy compounds. Finally, with reactive immunization, it might be possible to install an immune repertoire that reacts chemically with foreign pathogens by attacking critical residues such as the asparagine side chain or even the peptide bond itself.

REFERENCES AND NOTES

1. R. A. Lerner, S. J. Benkovic, P. G. Schultz, *Science* **252**, 659 (1991).
2. J. Guo, W. Huang, T. S. Scanlan, *J. Am. Chem. Soc.* **116**, 6062 (1994); P. Wirsching, J. A. Ashley, S. J.

Benkovic, K. D. Janda, R. A. Lerner, *Science* **252**, 680 (1991); S. J. Benkovic, J. A. Adams, C. L. Borders Jr., K. D. Janda, R. A. Lerner, *ibid.* **250**, 1135 (1990).

3. R. B. Silverman, *Mechanism-Based Enzyme Inactivation: Chemistry and Enzymology* (CRC Press, Boca Raton, FL, 1988), vols. 1 and 2; N. Seiler, M. J. Jung, J. Koch-Weser, Eds., *Enzyme-Activated Irreversible Inhibitors* (Elsevier–North Holland, Amsterdam, 1978); C. Walsh, *Tetrahedron* **38**, 871 (1982).
4. N. S. Sampson and P. A. Bartlett, *Biochemistry* **30**, 2255 (1991); P. A. Bartlett and L. A. Lamden, *Bioorg. Chem.* **14**, 356 (1986); A. J. J. Ooms and C. van Dijk, *Biochem. Pharmacol.* **15**, 1361 (1966).
5. J. Oleksyszyn and J. C. Powers, *Biochemistry* **30**, 485 (1991). (We used the diphenyl ester analog of **1** in another study and obtained 29 antibodies, but none showed any chemical reactivity with **4**.)
6. I. M. Kovach, A. J. Bennet, J. A. Bibbs, Q. Zhao, *J. Am. Chem. Soc.* **115**, 5138 (1993); I. M. Kovach, M. Larson, R. L. Schowen, *ibid.* **108**, 5490 (1986).
7. Compound **1** was synthesized from dimethyl 4-nitrobenzylphosphonate [H. Scherer, A. Hartmann, M. Regitz, B. D. Tunggal, H. Günther, *Chem. Ber.* **105**, 3357 (1972)] as follows: step 1, bromotrimethylsilane (TMSBr) and then oxalyl chloride, catalytic (cat.) di- methylformamide (DMF); step 2, addition of **15** [F. G. Bordwell and P. J. Boutan, *J. Am. Chem. Soc.* **79**, 717 (1957); F. G. Bordwell and G. D. Cooper, *ibid.* **74**, 1058 (1952)] and triethylamine (NEt_3); step 3, hydrogenation with palladium on carbon; step 4, glutaric anhydride. Compounds **4** and **5** were prepared as for **1**, except that in step 2 phenol or **15** was used, respectively, and in step 4, the reagents acetyl chloride and NEt_3. Compound **6** was synthesized from diethyl 4-aminobenzyl phosphonate (commercial) as follows: step 1, $NaNO_2$ and 6 M HCl, then NaN_3; step 2, TMSBr then oxalyl chloride with cat. DMF; step 3, *p*-nitrophenol and NEt_3; step 4, $SnCl_2$ and tetrahydrofuran; step 5, acetyl chloride and NEt_3, with silica gel purifications and recrystallizations as needed.
8. Compound **1** (5 μmol) was activated for coupling in DMF (50 μl) with an aqueous solution of 1-(3-dimethylaminopropyl)-3-ethylcarbodiimide (EDC) (6.5 μmol) and N-hydroxysulfosuccinimide (sulfo-NHS) (6.5 μmol). The mixture (aqueous content, 10 percent) was held for 20 hours at 22°C, and then added to KLH (5 mg) in 950 μl of 50 mM phosphate buffer, pH 7.5. This mixture was kept at 4°C for 18 hours during which time turbidity developed. The same procedure yields a nonturbid bovine serum albumin (BSA) conjugate. [The decomposition was estimated on the basis of the observed rate constant for hydrolysis (Table 1) and on the assumption that the stability of the compound free in solution and as a haptenic determinant was similar.] Immediately after conjugation, we immunized 129GIX$^+$ strain mice.
9. G. Kohler and C. Milstein, *Nature* **256**, 495 (1975). The hybridomas were derived from fusions with an SP2/0 myeloma cell line that retained the capacity to produce γ_{2b} and κ chains. Binding studies, cDNA sequencing, and NH_2-terminal protein sequencing indicated that each antibody contained one functional combining site of B-cell origin and one nonfunctional site that originated from the myeloma. All mAbs were purified from ascites to >95 percent homogeneity as follows: step 1, saturated ammonium sulfate; step 2, DEAE Sephacel (Pharmacia) chromatography; step 3, protein G affinity chromatography; step 4, Mono Q (Pharmacia) anion exchange chromatography.
10. SPO mAbs were stored in 100 mM Bicine, pH 8.0 at 4°C, and their concentrations were determined from an ultraviolet absorbance assay [ε_{280} = 1.35 (mg/ml)$^{-1}$ cm^{-1}] and an assumed molecular mass of 150 kD for immunoglobulin G (IgG). Both equilibrium and fluoresence binding studies were conducted in 100 mM Bicine, pH 8.0 [M. W. Steward, in *Handbook of Experimental Immunology*, D. M. Weir, Ed. (Blackwell, Oxford, ed. 4, 1986), vol. 1, chap. 25]. Compound **12** was synthesized from commercially available diethyl 4-aminobenzyl phosphonate as follows: step 1, trifluoroacetic anhydride; step 2, TMSBr then oxalyl chloride with cat. DMF; step 3, benzyl alcohol and NEt_3; step 4, PCl_5; step 5, addition of **15** and NEt_3; step 6, $NaBH_4$ and ethanol; step 7, acetyl chloride and NEt_3; step 8, hydrogenation with palladium on carbon. Silica gel purifications or recrystallizations were performed when needed. Compound **13** was prepared as above and compound **7** as in (*7*) except that [^{3}H]acetic anhydride (Amersham; 4 Ci/mmol) was used in place of acetyl chloride. These compounds were obtained with specific activities of 0.3 to 0.5 Ci/mmol. Compounds **8** and **14** were used for routine studies and were obtained in the same way as above with 1-[*carbonyl*-^{14}C]acetyl chloride (American Radiolabeled Chemicals; 55 mCi/mmol) with specific activities of 2 to 8 mCi/mmol.
11. Compound **16** was synthesized from dimethyl 4-nitrobenzyl phosphonate (*7*): step 1, PCl_5; step 2, addition of **15** and NEt_3; step 3, hydrogenation with palladium on carbon; step 4, acetyl chloride and NEt_3. Silica gel purifications or recrystallizations were performed when needed.
12. The mAbs were incubated in 100 mM Bicine, pH 8.0, 5 percent DMF in 5 percent CH_3CN (acetonitrile) cosolvent (total volume, 1 ml) in the presence of a 100 times molar excess of **7** or **8** for 1 hour and dialyzed with seven 200-ml portions of buffer with Slide-A-Lyzer cassettes (Pierce) for 48 hours. The proteins were then denatured as follows (i) 65°C, 15 minutes; in either 100 mM Bicine, pH 8.0, or 100 mM ammonium acetate, pH 5.5; (ii) 3.5 M KSCN, pH 6, 200 ml for 18 hours at 22°C; (iii) 8 M urea, pH 7, 200 ml for 18 hours at 22°C; (iv) 6 M guanidine-HCl, pH 5, for 18 hours at 22°C; (a) 1:1 (v/v) or (b) 200 ml; (v) 6 M guanidine-HCl in 5 percent perchloric acid, pH 1 to 2, 1:1 (v/v) for 5 minutes at 22°C. Only conditions (ii), (iv, b), and (v) resulted in a total loss of protein-bound radioactivity; otherwise, up to 80 percent of the protein-bound radioactivity remained. All dialyses were done with 100 mM ammonium acetate, pH 5.5.
13. J. H. Keijer, G. Z. Wolring, L. P. A. De Jong, *Biochim. Biophys. Acta* **334**, 146 (1974); L. W. Harris, J. H. Fleisher, J. Clark, W. J. Cliff, *Science* **154**, 404 (1966).
14. All reactions were done in 100 mM Bicine, pH 8.0, 5 percent DMF in 5 percent CH_3CN cosolvent at 22°C in the presence of mAb at 40 μM, or in its absence. Reactions were initiated by the addition **5** in DMF. Typical reaction volumes were 200 to 500 μl. At appropriate times, 30-μl portions were removed and quenched into 5 μl of aqueous 21 percent perchloric acid. Immediately, aqueous 6 M guanidine hydrochloride (25 μl), which contained 100 μM acetanilide as an external standard, was added. The final quenched solution was vortexed and held for at least 5 minutes before a 50-μl sample was analyzed by reversed-phase C_{18}-HPLC (VYDAC 201TP54). We monitored the reaction by following the formation of **12** and **15** at a detector setting of 254 nm and using an isocratic mobile phase of 9 percent CH_3CN and 91 percent water (0.1 percent trifluoroacetic acid) at 2.0 ml/min. The product concentrations from reactions were determined by comparison of peak height and area ratios (relative to acetanilide) against calibrated ratios of product standards. Background values were subtracted at each time point for all reactions.
15. The inactivation reaction was monitored spectrophotometrically by our following the release of **15** [ε_{266} = 13,360 M^{-1} cm^{-1}; 100 mM Bicine, pH 8.0, 5 percent DMF in 5 percent CH_3CN cosolvent]. No significant change in absorbance was detected; the products remained bound as a complex at the active site of the antibody from which **15** was slowly released, as confirmed by product concentrations from HPLC and comparison with reference standards and known amounts of **5**, which was hydrolyzed without antibody. Accurate values from antibody-catalyzed reactions could only be obtained after exposure to strongly denaturing conditions.
16. The progress curve data were fit to the following equation, which is a general expression for any mechanism of inhibition in which the steady state is reached by a first-order process.

$$P = vst + [(v_i - v_s)(1 - e^{-kt})/k] + d$$

where P is the product concentration, v_i is the initial velocity, v_s is the steady-state velocity, k is the observed first-order rate constant for approach to steady state, and d is the displacement of P from zero at t = 0 [J. F. Morrison and C. T. Walsh, *Adv. Enzymol.* **61**, 201 (1988)].
17. Both steady-state reactions and pre–steady-state stopped-flow experiments gave no indication of a "burst" of product release under conditions in (*15*). SPO71A7 showed similar behavior, whereas SPO50C1 showed a characteristic burst of one equivalent of **15** (k_{obs} = 1.8 s^{-1}). However, catalyzed hydrolysis of **18** by SPO49H4 or SPO71A7 was not significantly inhibited by addition of **15**. When SPO49H4 (1.0 nmol) or SPO71A7 (1.0 nmol) was mixed with a molar excess (×100) of **19** (4.30 mCi/mmol), then rapidly dialyzed (Slide-A-Lyzer cassettes; Pierce) into 100 mM ammonium acetate, pH 5.5, and then dialyzed extensively, the bound radioactivity corresponded to the incorporation of 1.0 nmol of ^{14}C label.
18. Two antibodies, SPO91B4 and SPO96G2, showed no reactivity with **5**, were not labeled with **19**, yet were good catalysts for the hydrolysis of **18**. These antibodies were probably elicited primarily through selection by **10** and operate via the principle of transition-state stabilization.
19. Tyrosine is the most likely candidate for antibody reactions involving covalent catalysis because of its frequency of occurrence at combining sites and its reactivity. A pH-rate profile for SPO49H4 was analyzed from pH 6.5 to 8.5 and was linear, thus excluding histidine. At higher pH, data could not be accurately acquired because of the high velocities, but the rapid turnover of **18** would preclude an amide intermediate derived from lysine. However, data for SPO71A7 were obtained up to pH 10.2 and gave a biphasic profile with a pK_a = 9.09, characteristic of tyrosine. For the reaction of *p*-cresol with **5** in 100 mM Bicine, pH 8.0, 5 percent DMF in 5 percent CH_3CN as cosolvent at 22°C, k_{obs} = 1.06 × 10^{-4} min^{-1} and the for *p*-cresol hydrolysis from **24**, k_{obs} = 5.37 × 10^{-6} min^{-1}. These were compared with the limits set by the k_{inact} of 6.4 min^{-1}. Similar data for ethanol and **17** were 3.7 × 10^{-7} min^{-1} and 7.2 × 10^{-8} min^{-1}, respectively. This would give rate enhancements at the diffusion limit, which is improbable and tends to rule out a serine residue.
20. The reactions were done in 100 mM Bicine, pH 8.0, 5 percent DMF in 5 percent CH_3CN cosolvent with 1.0 μM SPO49H4, 75 μM **18**, and varying concentrations of **5** at 22°C in 1-ml (1 cm) quartz cuvettes. The rates were monitored by the increase in absorbance at 266 nm because of the formation of **15** [ε_{266} = 13,360 M^{-1} cm^{-1}]. Reactions were done singly in a Shimadzu UV2100 equipped with an automatic cell changer and Peltier temperature control. For example, all cuvettes were filled with 883 μl of buffer, 35 μl of CH_3CN, and appropriate amounts of DMF. After temperature equilibration, a 15-μl sample of **18** (5.0 mM stock solution in CH_3CN) was added, and then immediately a sample of **5** (0.2 to 1.0 mM stock solutions in DMF) and 17 μl of SPO49H4 (59 μM stock solution in 100 mM Bicine, pH 8.0) were added. The solution was mixed within 7 seconds (Mini-Mix; Precision Cells, Inc.), auto-zeroed, and followed for 3 minutes. The spontaneous rate of hydrolysis of **18** was subtracted from all reactions. The concentrations of antibody, substrate, and inhibitor were adjusted to give pseudo first-order kinetics while remaining within acceptable limits of substrate depletion. The mathematics has been addressed (*21*). For our experiment, we also considered absolute concentrations of antibody and inhibitor and inhibitor decomposition. The compound **5** contained 0.2 percent of **12**. First, to avoid significant initial inhibition, we kept the antibody concentration to 1.0 μM and inhibitor concentrations to a maximum of 50 μM. Second, the reaction was followed for a period during which there was no significant hydrolysis of **5**. We could estimate production of **12** was 0.01 to 0.04 μM from spontaneous hydrolysis. For all reactions, total absorbance did not exceed 1.0 absorbance units.
21. S. G. Waley, *Biochem. J.* **227**, 843 (1985); W.-X. Tian and C.-L. Tsou, *Biochemistry* **21**, 1028 (1982); G. J. Hart and R. D. O'Brien, *Biochemistry* **12**, 2940 (1973).
22. The **15** is produced from consecutive first-order steps where there was no separation of rates. The

data can be fit to a double-exponential expression, but this gives no information as to correspondence between rate constants and the steps involved.
23. The pseudo first-order rate constants for hydrolysis of **15** from **17** and **24** were 4.33×10^{-6} min^{-1} and 3.55×10^{-5} min^{-1}, respectively.
24. After incubation of either SPO56C4 or SPO45G6 (5 nmol) with **7** (400 nmol; 11.5 mCi/mmol) in 100 mM Bicine, pH 8.0, 5 percent DMF in 5 percent CH_3CN cosolvent for 30 hours, denaturation at condition (v) in (12), and dialysis, the protein-bound radioactivity corresponded to 5 nmol of ^3H-label.
25. I. M. Kovach, *J. Enzyme Inhibition* **2**, 199 (1988).
26. Y. Ashani and B. S. Green, "Chemical Approaches to Understanding Enzyme Catalysis: Biomimetic Chemistry and Transition-State Analogs," *Proceedings of the 26th Oholo Conference*, Zichron Yaacov, Israel, 22 to 25 March 1981; B. S. Green, Y. Ashani, D. Chipman, Eds., *Studies in Organic Chemistry* (Elsevier, Amsterdam, 1981), vol. 10, p. 1.
27. O. Exner, *Correlation Analysis of Chemical Data* (Plenum Press, New York, 1988); C. D. Johnson, *The Hammett Equation* (Cambridge Univ. Press, Cambridge, 1973); O. Exner, in *Advances in Linear Free Energy Relationships*, N. B. Chapman and J. Shorter, Eds. (Plenum, New York, 1972).
28. J. F. Kirsch, in *Advances in Linear Free Energy Relationships*, N. B. Chapman and J. Shorter, Eds. (Plenum Press, New York, 1972); R. E. Williams and M. L. Bender, *Can. J. Biochem.* **49**, 210 (1971); A. Williams, *Biochemistry* **9**, 3383 (1970); M. L. Bender and K. Nakamura, *J. Am. Chem. Soc.* **84**, 2577 (1962).
29. R. A. Gibbs, P. A. Benkovic, K. D. Janda, R. A. Lerner, S. J. Benkovic, *J. Am. Chem. Soc.* **114**, 3528 (1992).
30. W. J. Donarski, D. P. Dumas, D. P. Heitmeyer, V. E. Lewis, F. M. Raushel, *Biochemistry* **28**, 4650 (1989); A. M. Relimpio, *Gen. Pharmacol.* **9**, 49 (1978); J. W. Hovanec and C. N. Lieske, *Biochemistry* **11**, 1051 (1972); E. L. Becker, *Biochim. Biophys. Acta* **147**, 289 (1967); T. R. Fukuto and R. L. Metcalf, *J. Agr. Food Chem.* **4**, 930 (1956).
31. The antibody required the *p*-SO_2Me phenyl ring for activation of a substrate. Other symmetrically substituted compounds bound poorly or showed minimal reactivity. For example, the rather stable analog **4** gave no detectable antibody-catalyzed reaction, no competitive inhibition compared at an equivalent concentration of the mixed-ester counterpart **25**, and a $K_d > 100$ μM, as determined by fluorescence quenching. Even the highly reactive phosphonate **9** (stability similar to **5**) had a k_{obs} that was only 1 percent that of **5**. Compounds **22** to **31** were synthesized as described (*7*).
32. In reactions with antibody, 40 μM SPO49H4 and 700 μM substrate were used, except for **29** where the substrate was 500 μM because of solubility limitations. All conditions and analyses for background and antibody-catalyzed reactions were as in (*14*) except that 3-fluoroacetanilide was the external standard during assays with **30**.
33. A value of 1.0, intermediate between $\sigma = 0.78$ and $\sigma^- = 1.27$, was used for the nitro group (*36*). For our data, σ^- gave a slightly better correlation, but with very similar results ($\rho = 0.80$, $r = 0.98$). The deviant behavior of **5**, **22**, **23**, and **30** relative to σ or σ^- suggests a complex interdependence of mesomeric and inductive effects.
34. The observed product distributions were controlled by the electron-withdrawing character of the *p*-SO_2Me group. This functionality, at least in these compounds, is competitive with the nitro group. Although the k_{hyd} for **31** is slightly greater than that of **5**, the partitioning actually favors formation of **15** by 52 versus 48 percent. The ratios for **27** to **30** cluster at 60 to 70 percent versus 40 to 30 percent, and for **22** to **26** at 80 to 90 percent versus 20 to 10 percent. Whether the mechanism depends on in-line displacement or adjacent attack with pseudorotation via true trigonal bipyramidal intermediates, or back side S_N2-type attack with inversion through a quasi-trigonal-bipyramidal transition state is uncertain. However, in that apical attack and departure are favored, the lack of steric bias for attack and the apicophilicities of the ligands involved suggest that pseudorotational "leakage" from pentavalent intermediates is possible.
35. Catalyzed formation of **15** (about 40 percent) was observed only for compound **31** during the reaction.
36. J. F. Kirsch, W. Clewell, A. Simon, *J. Org. Chem.* **33**, 127 (1968); T. C. Bruice and S. J. Benkovic, *J. Am. Chem. Soc.* **86**, 418 (1964); T. C. Bruice and M. F. Mayahi, *J. Am. Chem. Soc.* **82**, 3067 (1960); T. C. Bruice and G. L. Schmir, *J. Am. Chem. Soc.* **79**, 1663 (1957).
37. A large ρ of 2 to 3 in phenyl ester hydrolysis is characteristic of nucleophilic attack by a neutral nitrogen nucleophile such as imidazole (*29, 36*). However, large ρ values in enzyme-catalyzed reactions of phosphonate or phosphate esters apparently can arise in other ways. From data in (*30*), it could be estimated that the serine of acetylcholinesterase or the metal hydroxide of the phosphotriesterase from *Pseudomonas diminuta* gave ρ = 2 to 2.5 in their reactions. These enzymatic reactions are also indicative of a phenoxide-like transition state with rate-determining P-O bond cleavage. This contrasts with the nonenzymatic, general-base catalyzed hydrolysis of reactive phosphonates, which are characterized by early transition states and rate-determining P-O bond formation (*6*). Although the magnitude of ρ found for SPO49H4 does not, in itself, demand an antibody nucleophile, it is consistent with the required transition state. In light of other evidence, the ρ value supports a mechanism of covalent catalysis.
38. Displacement reactions at phosphorus centers are more complex than nucleophilic addition to a carbonyl carbon because of the extra ligand. Rapid interconversion of the pentavalent intermediates (pseudorotation) formed along the reaction coordinate can occur if the electronic properties of the ligands are not too different as in phosphate esters [G. R. J. Thatcher and R. Kluger, *Adv. Phys. Org. Chem.* **25**, 99 (1989); S. J. Benkovic and K. J. Schray, in *Transition States of Biochemical Processes*, R. D. Gandour and R. L. Schowen, Eds. (Plenum, New York, 1978)]. Although the behavior of phosphonate esters has been less studied, it seems that permutational isomerization is not as common [I. M. Kovach and D. Huhta, *Theochem* **79**, 335 (1991); I. M. Kovach, D. Huhta, S. Baptist, *ibid.* **72**, 99 (1991)]. Loss of the *p*-substituted phenols by hydroxide attack would require an adjacent addition with pseudorotation, which is unprecedented in enzymology. However, attack of an active-site serine in an in-line mechanism with pseudorotation was implicated in the inactivation of α-lytic protease [N. S. Sampson and P. A. Bartlett (*4*)].
39. W. W. Cleland, *Methods Enzymol.* **63A**, 103 (1979).
40. We thank L. Tucker, G. P. McElhaney, M. Sakurai, D. M. Kubitz, and L. Bibbs for technical assistance; K. Cole-Moore, J. Hightower, and P. Myer for help in the preparation of the manuscript. Supported by NIH Program Project Grant PO1 CA27489-16 (R.A.L. and K.D.J.), NIH GM48351 (K.D.J.), National Institute on Drug Abuse DA08590 (K.D.J.), and an A. P. Sloan Foundation fellowship (K.D.J.).

15 June 1995; accepted 1 November 1995